Supplemental Figure 1

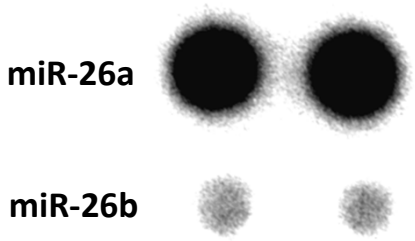

Supplemental Figure 1. Expression of miR-26a is higher than miR-26b in the mouse liver. Dot blot analysis of miR-26a/b expression in the livers of wild-type mice fed a chow diet (CD).

Supplemental Figure 2

Gene ontology analysis

Term	Count	p value
cellular metabolic process	92	2.62E-04
cellular process	128	6.83E-04
primary metabolic process	92	0.001488
cellular macromolecule metabolic process	73	0.002241
negative regulation of cell proliferation	11	0.004752
gene silencing by RNA	4	0.004894
DNA metabolic process	13	0.006998
protein localization	18	0.010977
negative regulation of biological process	30	0.012601
metabolic process	95	0.013085

Supplemental Figure 2. Potential involvement of miR-26a in metabolism. KEGG pathway analysis on Top 500 targets of miR-26a predicted by TargetScan.

Supplemental Figure 3

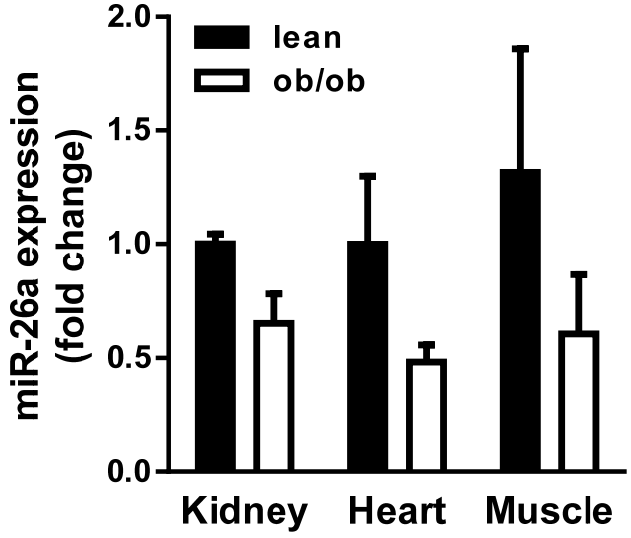

Supplemental Figure 3. miR-26a is slightly reduced in obesity-associated organs of ob/ob mice. QRT-PCR analysis of miR-26a expression in kidney, heart and muscle of ob/ob mice. Data are shown as mean ± SEM.

Supplemental Figure 4

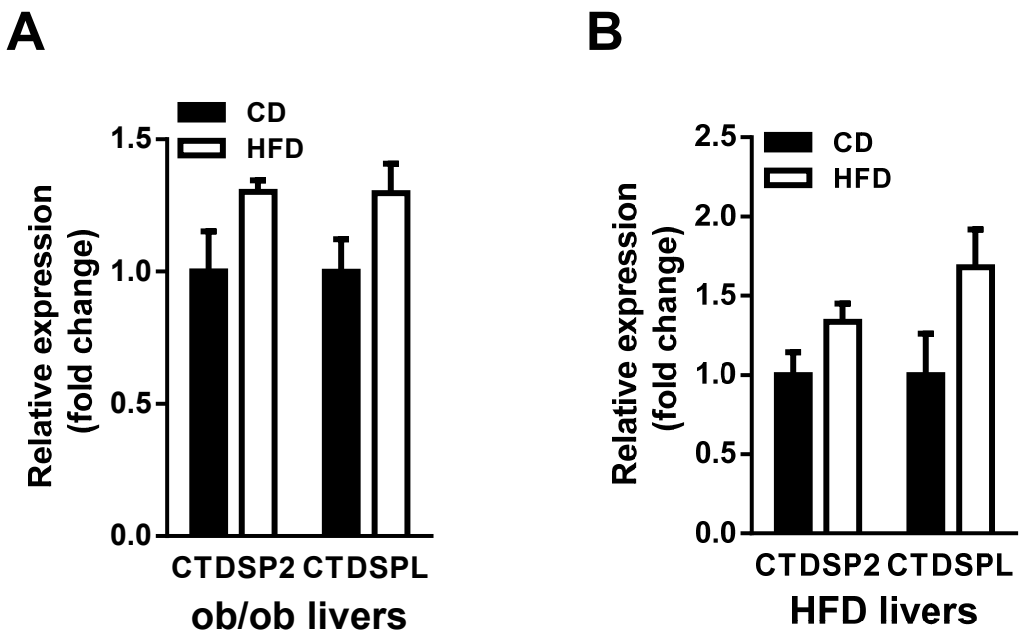

Supplemental Figure 4. Expression of miR-26a host genes, CTDSP2 and CTDSPL, is not affected by obesity. (**A** and **B**) QRT-PCR analysis of miR-26a expression in the livers of ob/ob (**A**) and high fat diet (HFD)-induced obese mice (**B**). Data are shown as mean ± SEM.

Supplemental Figure 5

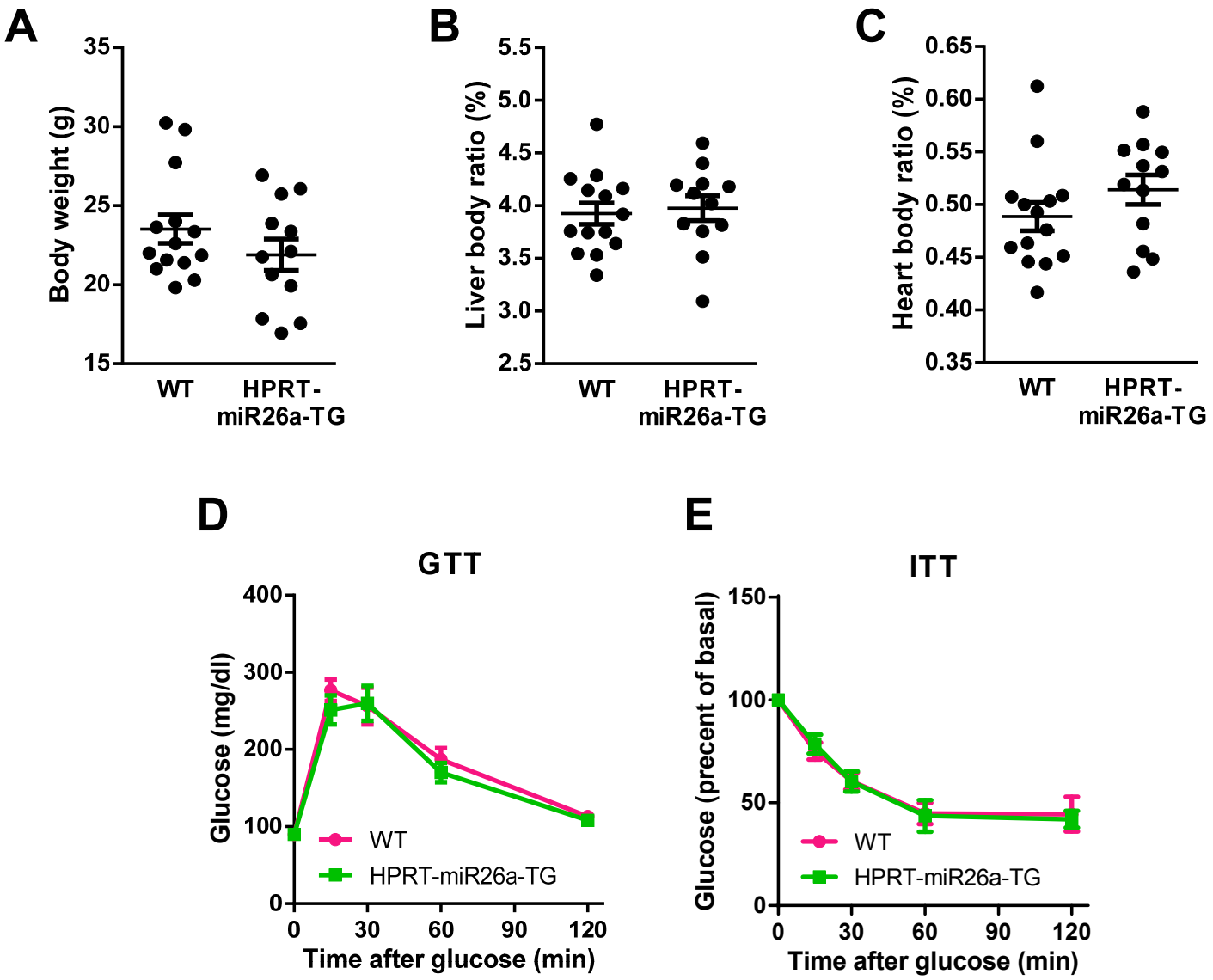

Supplemental Figure 5. HPRT-miR-26a TG and WT mice fed a CD have no significant differences in body weight (BW), organ weight, glucose disposal or insulin sensitivity **.** (**A-E**) Adult (8-12 weeks old) male HPRT-miR26a-TG mice and their WT littermate controls fed a chow diet were studied. Body weight (**A**), ratio of liver (**B**) and heart (**C**) to body weight were measured (HPRT-miR26a-TG, n=12; WT, n=14). (**D**) GTT (HPRT-miR26a-TG, n=7; WT, n=7). (**F**) ITT (HPRT-miR-26a-TG, n=7; WT, n=7). Data are shown as mean ± SEM.

Supplemental Figure 6

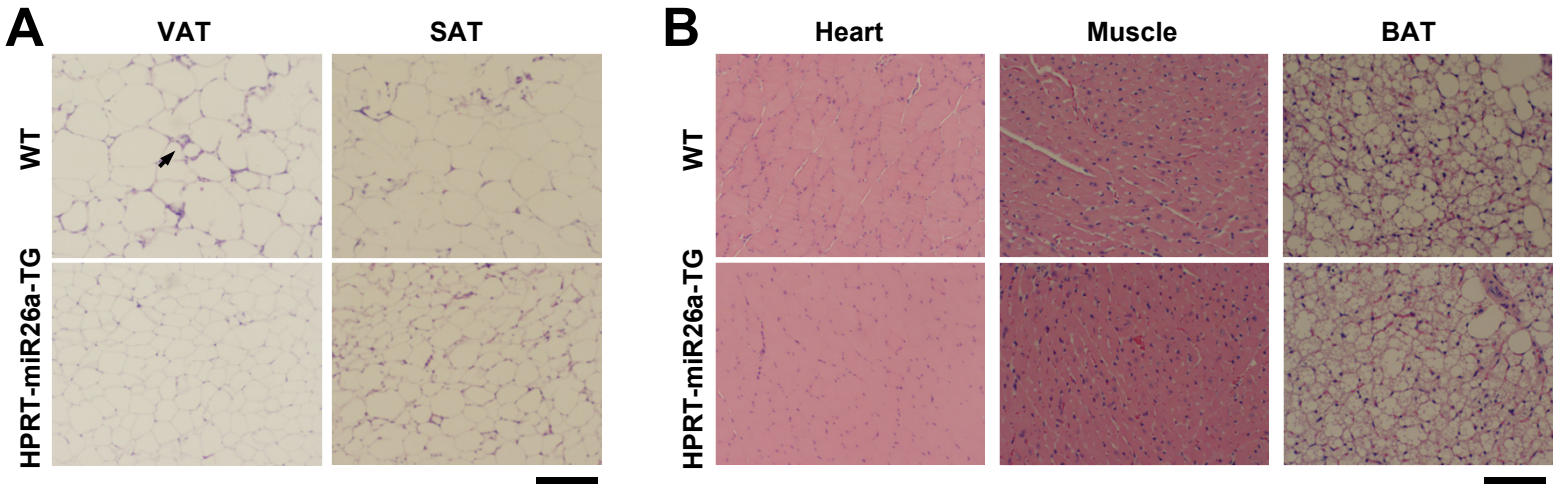

Supplemental Figure 6. Hematoxylin staining of paraffin sections from visceral (VAT) and subcutaneous (SAT) fat (**A**), heart, muscle and brown adipose tissue (BAT) (**B**) of HPRT-miR26a-TG and WT mice fed an HFD for 18 weeks. Scale bar, 100 μM.

Supplemental Figure 7

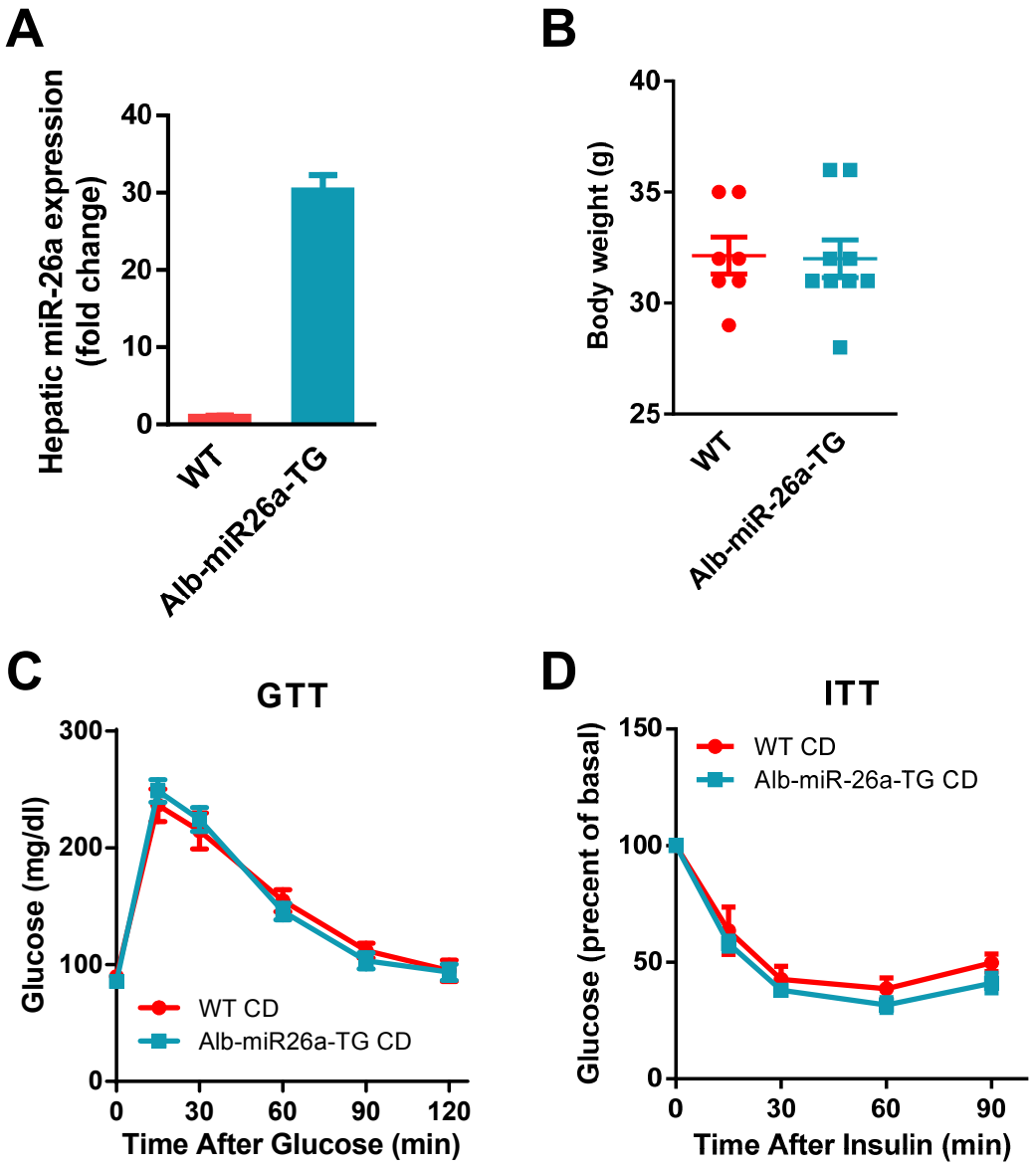

Supplemental Figure 7. Alb-miR-26a TG and WT mice fed a CD have no significant differences in glucose disposal or insulin sensitivity**.** (**A**) QRT-PCR analysis of miR-26a expression in liver of Alb-miR-26a TG and their WT littermate controls (n=6). (**B-D**) Adult (8-12 weeks old) male Alb-miR26a-TG mice and their WT littermate controls fed a chow diet were studied. (**B**) Body weight (Alb-miR26a-TG, n=9; WT, n=7), (**C**) GTT (Alb-miR26a-TG, n=4; WT, n=4), and (**D**) ITT (Alb-miR26a-TG, n=9; WT, n=6) were measured. Data are shown as mean ± SEM.

Supplemental Figure 8

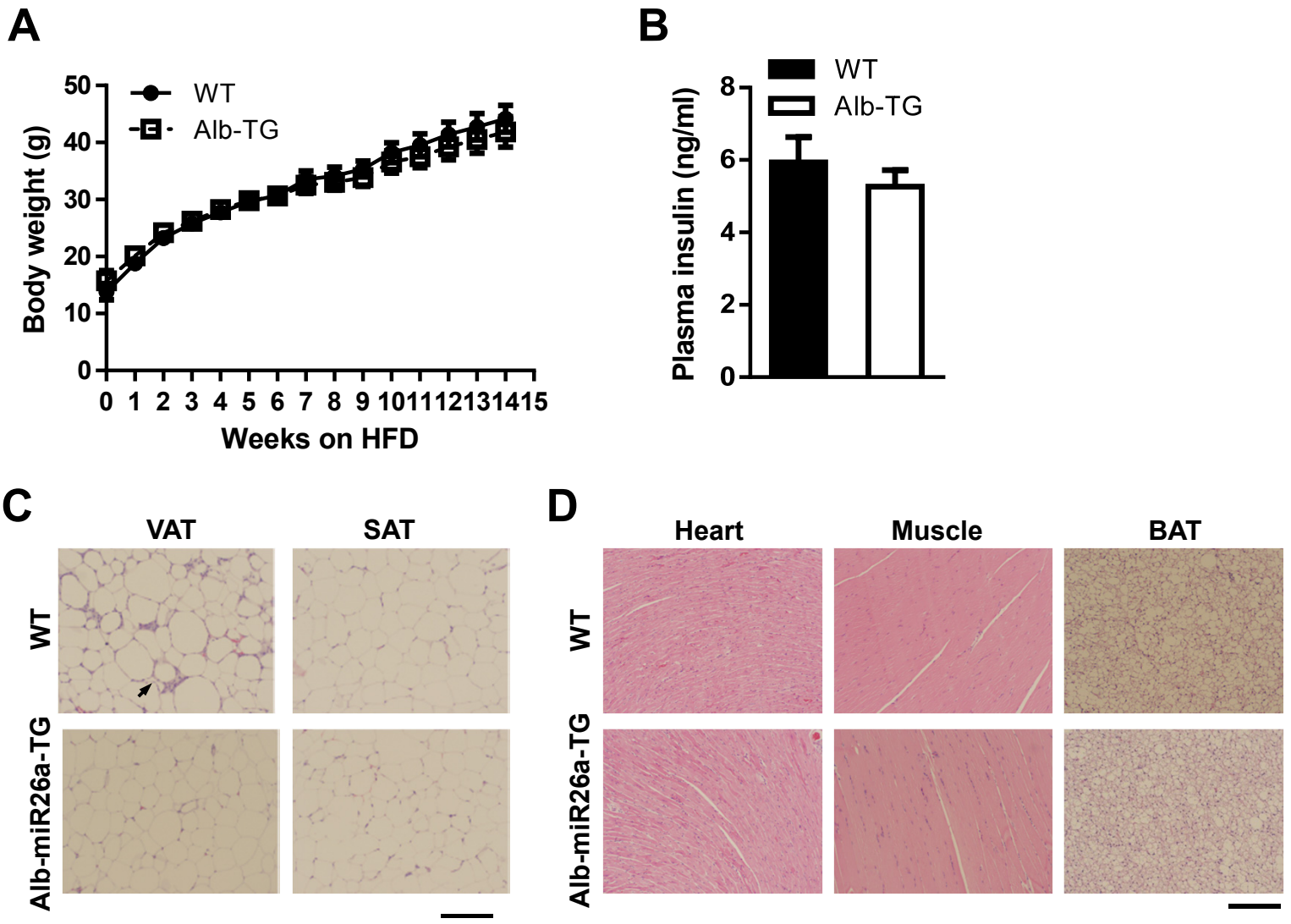

Supplemental Figure 8. Alb-miR-26a-TG and WT mice were fed HFD beginning at 6-8 weeks-of-age. The following measurements were performed during the course of the HFD. (**A**) Body weight (n=15-17). (**B**) Plasma insulin levels during GTT (30 minutes after glucose injection) (n=3). (**C** and **D**) Hematoxylin staining of paraffin sections from visceral (VAT) and subcutaneous (SAT) fat (**C**), heart, muscle and brown adipose tissue (BAT) (**D**) of Alb-miR-26a-TG and WT mice fed an HFD for 16 weeks. Scale bar, 100 μM.

Supplemental Figure 9

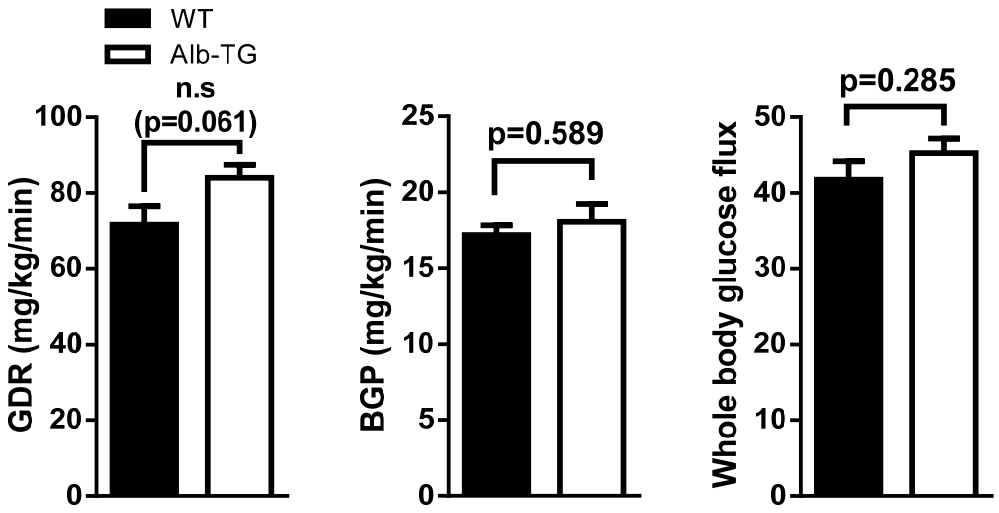

Supplemental Figure 9. Hyperinsulinemic-euglyemic clamp studies on Alb-miR-26a TG mice and WT controls after 18 weeks of HFD (n=4-6). GDR: glucose disposal rate; BGP: basal glucose production.

Supplemental Figure 10

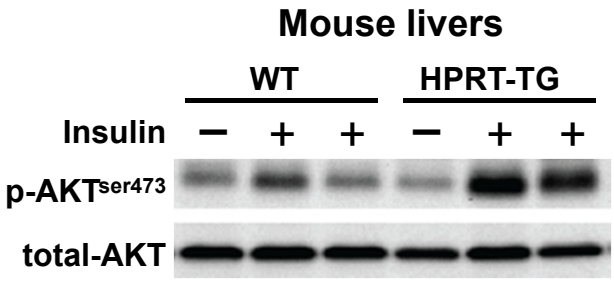

Supplemental Figure 10. AKT phosphorylation in livers of HPRT-miR-26a TG mice and WT littermate controls infused with insulin (0.25 U/kg) through the portal vein and fed an HFD for 18 weeks.

Supplemental Figure 11

Gene Ontology analysis

Gene Ontology term	Gene count	Fold enrichment	P Value
oxidation reduction	79	5.938286	2.57E-39
translation	34	5.383832	4.80E-15
generation of precursor metabolites and energy	29	5.612557	2.58E-13
fatty acid metabolic process	21	5.765072	6.05E-10
glucose metabolic process	17	6.133723	1.61E-08
hexose metabolic process	18	5.380084	3.90E-08
monosaccharide metabolic process	19	5.024855	4.26E-08
carboxylic acid catabolic process	13	8.107026	5.72E-08
organic acid catabolic process	13	8.107026	5.72E-08
energy derivation by oxidation of organic compounds	14	7.216144	6.17E-08
cofactor metabolic process	17	4.718248	6.31E-07
coenzyme metabolic process	14	4.94533	4.99E-06

Supplemental Figure 11. Gene ontology analysis of differentially expressed hepatic proteins between WT and Alb-miR-26a TG mice.

Supplemental Figure 12

KEGG pathway analysis

Term	Count	*P* Value
Fatty acid metabolism	**14**	**2.32E-11**
Ribosome	17	2.58E-10
PPAR signaling pathway	13	3.51E-07
Valine, leucine and isoleucine degradation	10	1.21E-06
Drug metabolism	12	1.59E-06
Metabolism of xenobiotics by cytochrome P450	10	2.69E-05
Propanoate metabolism	7	6.94E-05
Glycolysis / Gluconeogenesis	**9**	**2.21E-04**
Starch and sucrose metabolism	6	0.00165
Tryptophan metabolism	6	0.002664

Supplemental Figure 12. KEGG pathway analysis on hepatic proteins downregulated in Alb-miR-26a TG mice.

Supplemental Figure 13

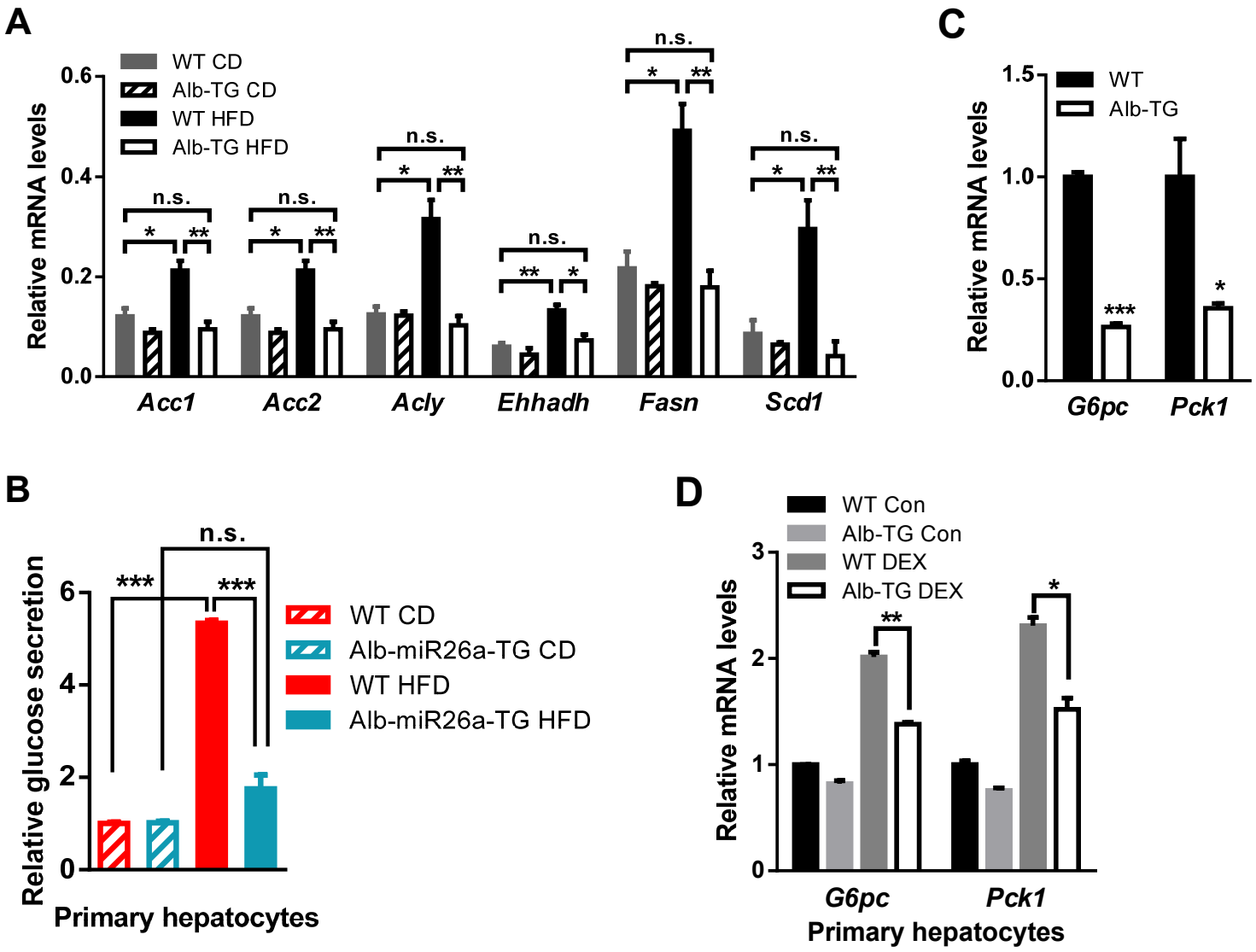

Supplemental Figure 13. (**A**) QRT-PCR analysis of selected lipogenic genes in livers from mice either fed a CD or HFD for 16 weeks (n=3-5 mice/group). (**B**) Glucose production (4 hours) in primary hepatocytes isolated from Alb-miR-26a TG and WT mice fed either a CD or an HFD for 16 weeks. Results are normalized to the level in hepatocytes isolated from WT mice fed a CD (n=3). (**C**) Expression of gluconeogenic genes in livers of 16 hours fasted Alb-miR-26a TG and WT mice fed a CD (n=3). (**D**) Expression of gluconeogenic genes in DEX-treated primary hepatocytes isolated from Alb-miR-26a TG and WT mice fed a CD (n=3). Data are shown as mean ± SEM. n.s., not significant.

Supplemental Figure 14

No. of miR-26a target sites		
	Hsa	Mmu
Acsl3	1	2
Acsl4	2	2
GSK3β	3	3
Pck1	1	1
Pkcδ	1	1
Pkcθ	1	2
Tcf7l2	1	1

Supplemental Figure 14. Number of predicted miR-26a target sites for indicated genes.

Supplemental Figure 15

Supplemental Figure 15. miR-26a targets murine Acsl3, Acsl4, Gsk3β, Pck1, Pkcδ, Pkcθ and Tcf7l2. Predicted consequential pairing of target region, as well as its mutant, and miR-26a is shown (bottom).

Supplemental Figure 16

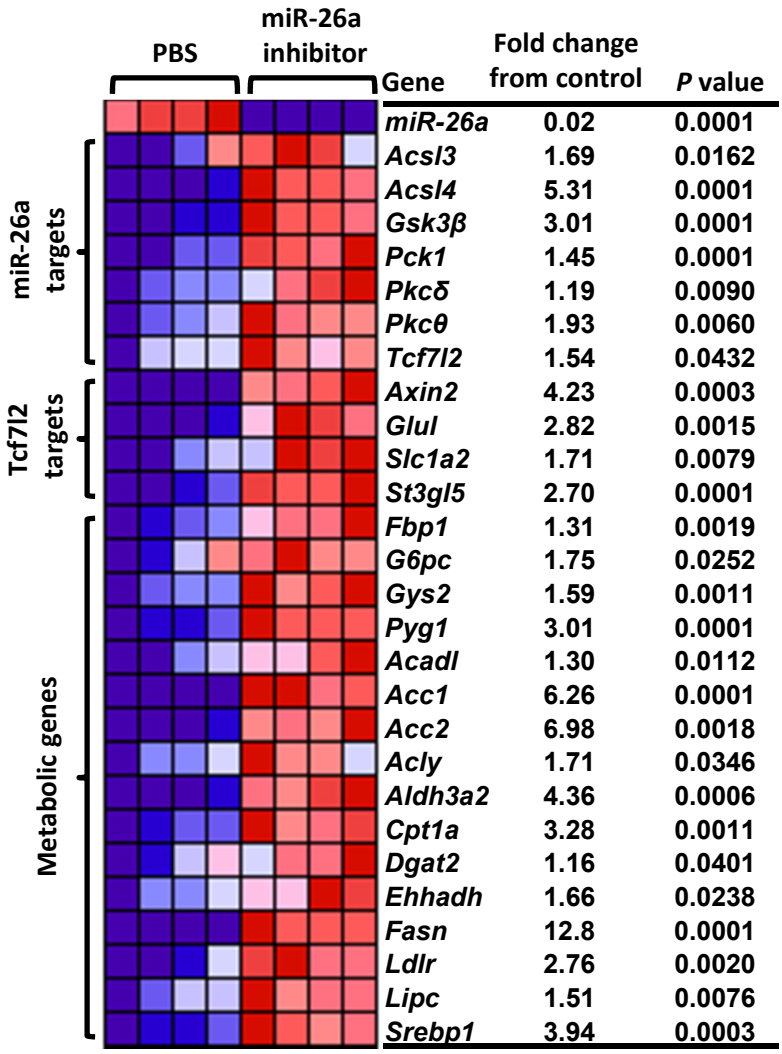

Gene	Fold change from control	*P* value
miR-26a	0.02	0.0001
Acsl3	1.69	0.0162
Acsl4	5.31	0.0001
Gsk3β	3.01	0.0001
Pck1	1.45	0.0001
Pkcδ	1.19	0.0090
Pkcθ	1.93	0.0060
Tcf7l2	1.54	0.0432
Axin2	4.23	0.0003
Glul	2.82	0.0015
Slc1a2	1.71	0.0079
St3gl5	2.70	0.0001
Fbp1	1.31	0.0019
G6pc	1.75	0.0252
Gys2	1.59	0.0011
Pyg1	3.01	0.0001
Acadl	1.30	0.0112
Acc1	6.26	0.0001
Acc2	6.98	0.0018
Acly	1.71	0.0346
Aldh3a2	4.36	0.0006
Cpt1a	3.28	0.0011
Dgat2	1.16	0.0401
Ehhadh	1.66	0.0238
Fasn	12.8	0.0001
Ldlr	2.76	0.0020
Lipc	1.51	0.0076
Srebp1	3.94	0.0003

Supplemental Figure 16. Heatmap of mRNA levels of hepatic genes in CD-fed WT mice that received a single injection of LNA-miR-26a antisense inhibitor or PBS (n=4). Red and blue depict higher and lower gene expression, respectively. Color intensity indicates magnitude of expression differences.

Supplemental Table 2

Gene Ontology analysis (related to Figure 4B)

Term	Genes
oxidation reduction	CYP2D9, CYP2J5, CYB5R3, CYP2D10, ACOX1, ASPDH, UQCRC1, EHHADH, PRDX5, PRDX2, PRDX3, UQCRFS1, PRDX1, AKR1C13, MTHFD1, PECR, UQCR10, CPOX, NDUFS8, SPR, DHTKD1, NDUFS2, RTN4IP1, NQO2, SUOX, CYP2C54, ACADM, CYP1A1, CYCS, CYP2C29, QDPR, CYB5B, GRHPR, ACADL, POR, DHRS1, DHRS4, CYP27A1, ALDH1B1, UQCRH, SQLE, DLD, HSD11B1, MECR, HSD17B11, ME1, ME3, ACADSB, HSD17B13, HSD17B12, UGDH, ADH5, AASS, FTH1, ALDH3A2, CYP4A12A, FMO1, FASN, IDH2, DMGDH, HSD17B4, BCKDHA, GPD2, NDUFA4, GCDH, CYP2C37, PTGR2, NDUFA9, MAOB, BCKDHB, HGD, CRYZ, SOD1, SLC25A12, CYP7B1, DBT, BLVRB, ACAD11, CYP4A14
translation	TUFM, RPL17, RPL14, RPLP2, RPS2, RPL7, RPS3A, RPLP0, RPL9, RPL3, RPL10, RPL10A, RPL4, RPS20, RPL12, RPS27A, RPS24, EEF1A1, AARS, RPL27, RPL24, RPS4X, EIF4G2, TARS, RPS18, RPL18A, RPL22, RPS17, RPS14, EIF4A2, RPL21, EIF4A1, RPS13, EEF1G
generation of precursor metabolites and energy	ALDOA, UQCRC1, ALDOB, PGAM1, AASS, UQCRFS1, TPI1, UQCR10, NDUFS8, IDH2, ENO3, GYS2, DHTKD1, NDUFS2, ENO1, NDUFA4, DLST, NDUFA9, SUCLG1, CYCS, CYB5B, PPP1CB, PCK1, SLC25A12, GBE1, PYGL, UQCRH, DLD, PYGB
fatty acid metabolic process	ACOX1, ACADSB, ECH1, ACADM, CPT2, EHHADH, ECHDC2, LYPLA2, LYPLA1, ACADL, CPT1A, PECR, TPI1, CYP4A12A, FAAH, FASN, HSD17B4, ACAA1B, MECR, SLC27A2, CROT
glucose metabolic process	ALDOA, GPD2, ALDOB, PGAM1, FBP1, PPP1CB, CPT1A, PCK1, PGLS, TPI1, GBE1, PYGL, ENO3, GYS2, DHTKD1, PYGB, ENO1
hexose metabolic process	ALDOA, GPD2, ALDOB, PGAM1, FBP1, PPP1CB, CPT1A, PCK1, GALK1, PGLS, TPI1, GBE1, PYGL, ENO3, GYS2, DHTKD1, PYGB, ENO1
monosaccharide metabolic process	GPD2, ALDOA, ALDOB, PGAM1, FBP1, PPP1CB, CPT1A, PCK1, GALK1, PGLS, UGT1A9, TPI1, GBE1, PYGL, UGT1A2, ENO3, GYS2, DHTKD1, PYGB, ENO1
organic acid catabolic process	BCKDHA, ACOX1, ACADM, EHHADH, BCKDHB, HGD, AASS, MTHFD1, AMDHD1, FAAH, DMGDH, HSD17B4, SLC27A2
carboxylic acid catabolic process	BCKDHA, ACOX1, ACADM, EHHADH, BCKDHB, HGD, AASS, MTHFD1, AMDHD1, FAAH, DMGDH, HSD17B4, SLC27A2
energy derivation by oxidation of organic compounds	DLST, UQCRC1, SUCLG1, PPP1CB, PCK1, SLC25A12, UQCR10, GBE1, UQCRH, PYGL, DLD, IDH2, GYS2, PYGB
cofactor metabolic process	ASPDH, DLST, COASY, ALAD, EHHADH, SUCLG1, GSTT1, SOD1, MTHFD1, DBT, PGLS, TPI1, HPX, CPOX, GSTK1, IDH2, QPRT
coenzyme metabolic process	DLST, COASY, ASPDH, EHHADH, SUCLG1, GSTT1, SOD1, MTHFD1, DBT, PGLS, TPI1, GSTK1, IDH2, QPRT